

Published in final edited form as:

*Angew Chem Int Ed Engl.* 2012 September 3; 51(36): 9132–9136. doi:10.1002/anie.201203602.

## Characterization of a Unique Thiolato-Iron(III)-Peroxide Complex

**Dr. Aidan R. McDonald,**

Department of Chemistry, University of Minnesota, 207 Pleasant Street SE, Minneapolis, MN 55455, USA

**Dr. Katherine M. Van Heuvelen,**

Department of Chemistry, University of Minnesota, 207 Pleasant Street SE, Minneapolis, MN 55455, USA

**Dr. Yisong Guo,**

Department of Chemistry, Carnegie Mellon University, 4400 Fifth Avenue, Pittsburgh, PA 15213, USA

**Dr. Feifei Li,**

Department of Chemistry, University of Minnesota, 207 Pleasant Street SE, Minneapolis, MN 55455, USA

**Prof. Dr. Emile L. Bominaar,**

Department of Chemistry, Carnegie Mellon University, 4400 Fifth Avenue, Pittsburgh, PA 15213, USA

**Prof. Dr. Eckard Münck, and**

Department of Chemistry, Carnegie Mellon University, 4400 Fifth Avenue, Pittsburgh, PA 15213, USA

**Prof. Dr. Lawrence Que Jr.**

Department of Chemistry, University of Minnesota, 207 Pleasant Street SE, Minneapolis, MN 55455, USA

Eckard Münck: emunck@cmu.edu; Lawrence Que: larryque@umn.edu

### Keywords

nonheme iron; superoxide reductase; iron-peroxo intermediates; iron-thiolate; aromatase; NO synthase

Thiolate ligation to iron plays a vital role in the enzymatic deactivation of reactive oxygen species. Superoxide reductase (SOR) found in microaerophilics catalyzes the reduction of superoxide ( $O_2^{\cdot-}$ ), yielding  $H_2O_2$ <sup>[1]</sup> and has an active site that consists of an iron center with four equatorial His ligands and an axial Cys ligand. The thiolate is proposed to stabilize the O–O bond of  $RS-Fe^{III}(\eta^1-OO(-/H))$  intermediates and to weaken the Fe–(OO) bond to facilitate formation of  $H_2O_2$ .<sup>[1,2]</sup> Evidence for an intermediate in the reaction between  $O_2^{\cdot-}$  and SOR has been obtained, which exhibits a visible absorption feature at ~600 nm.<sup>[3]</sup> Pulse radiolysis studies showed diffusion-controlled pH-independent formation of the intermediate, while its decay was found to be pH-dependent. These results led to the postulation of the intermediate as either an  $RS-Fe^{II}(OO\cdot)$  adduct or the isoelectronic  $RS-Fe^{III}(OO^-)$ ; however its short lifetime has made it difficult to establish the iron oxidation

Correspondence to: Eckard Münck, emunck@cmu.edu; Lawrence Que, Jr., larryque@umn.edu.

Supporting information for this article is available on the WWW under <http://www.angewandte.org> or from the author.

state experimentally. We have thus endeavored to obtain a synthetic analog of this intermediate.

A number of synthetic non-heme RS-Fe<sup>III</sup>( $\eta^1$ -OOX) (X = H, alkyl) complexes have been reported recently,<sup>[4]</sup> providing insights into the role thiolate ligation plays in modulating the reactivity of peroxide complexes, and the nature of the RS-Fe<sup>III</sup>( $\eta^1$ -OOH) intermediate observed in SOR (Table 1). However, there are no reports detailing the isolation of an RS-Fe<sup>III</sup>( $\eta^1$ -OO<sup>-</sup>) complex. Herein, we describe the spectroscopic characterization of a synthetic complex that serves to model the putative RS-Fe<sup>III</sup>( $\eta^1$ -OO<sup>-</sup>) intermediate found in SOR.

[Fe<sup>II</sup>(TMCS)]PF<sub>6</sub> (**1**) acts as an ideal mimic of the SOR active site because it contains four equatorial N ligands and an axial S bound to the iron center (Scheme 1).<sup>[5]</sup> **1** reacted with KO<sub>2</sub> (dissolved in pure DMF in the presence of 2 equiv. of 18-crown-6) at -90 °C in a 4:1 THF/DMF solvent mixture. The characteristic UV feature of **1** ( $\lambda_{\text{max}} = 320$  nm, Figure 1) disappeared over the course of 10 s and was replaced by two new intense features ( $\lambda_{\text{max}} = 460, 610$  nm), assigned to transient species **2**. The visible features achieved maximum intensity when an excess (>50-fold) of KO<sub>2</sub> was used. Intermediate **2** was reasonably stable at -90 °C, decaying over the course of ~ 3 h to produce **1** nearly quantitatively (Figure S1). **2** could then be regenerated by replenishing the KO<sub>2</sub>. These observations suggest that superoxide binding to **1** is reversible, with the decay of **2** presumably reflecting the loss of KO<sub>2</sub> due to its gradual disproportionation in the reaction medium and a shift of the equilibrium back to **1** (Scheme 1).<sup>[6]</sup> Similar chemistry has been reported for a crown-ether functionalized porphyrin ligand that facilitates the reversible formation of a heme-Fe<sup>III</sup>(OO) complex from the heme-Fe<sup>II</sup> precursor and KO<sub>2</sub>.<sup>[7]</sup>

The highly chromophoric nature of **2** suggests that the iron center has been oxidized to Fe<sup>III</sup>, concomitant with the reduction of the superoxide ligand to the peroxide level. However the electronic absorption spectrum of **2** is quite distinct from those reported for related non-heme RS-Fe<sup>III</sup>(OOX) (X = H or alkyl) complexes (Table 1). While all complexes exhibit broad absorption features in the 500–800 nm region typically associated with peroxo-to-Fe<sup>III</sup> charge transfer transitions, **2** has an additional feature at 460 nm ( $\epsilon = 6100 \text{ M}^{-1}\text{cm}^{-1}$ ) that is sharper and more intense (Figure 1). For comparison, treatment of [Fe<sup>II</sup>(TMC)(OTf)]<sup>+</sup> with KO<sub>2</sub> afforded a product with a broad band at 850 nm (Figure S2), nearly identical to that observed for [Fe<sup>III</sup>(TMC)( $\eta^2$ -OO)]<sup>+</sup> in CH<sub>3</sub>CN at -40 °C.<sup>[8]</sup> It would thus appear that the more basic axial ligand of **2** is required to elicit its novel absorption features. We therefore postulate that **2** represents a thus far unprecedented example of an RS-Fe<sup>III</sup>( $\eta^1$ -OO<sup>-</sup>) complex.

EPR spectra of **2** revealed broad features belonging to an  $S = 5/2$  species (Figure 1, inset). The spectra indicate that the rhombicity parameter, E/D, is distributed around a mean value of E/D  $\approx$  0.08. The gray curve is an illustrative simulation for the major contributing species: the feature at  $g = 7.9$  belongs to the  $M_S = \pm 1/2$  ground doublet and the resonance  $g = 5.75$  results from the  $M_S = \pm 3/2$  excited state. The feature marked with the star is a minor rhombic contaminant ( $\approx$  0.5% of total Fe) (see Figure S5 for more details).<sup>[8b]</sup> The  $S = 5/2$  species could arise from a ferromagnetically coupled [ $S_{\text{Fe(II)}} = 2/S_{\text{superoxide}} = 1/2$ ] center or from a high-spin Fe<sup>III</sup>-peroxide complex. The <sup>57</sup>Fe magnetic hyperfine interactions as well as the isomer shift of **2**, obtained from Mössbauer spectra (Figure 2) establish that the iron center is in the high-spin ferric state.

We have simulated the 4.2 K Mössbauer spectra of **2** using the  $S = 5/2$  spin Hamiltonian (parameters listed in the caption of Figure 2)

$$\mathcal{H} = D(S_z^2 - 3S^2/4) + E(S_x^2 - S_y^2) + \beta \mathbf{S} \cdot \mathbf{g} \cdot \mathbf{B} + \mathbf{S} \cdot \mathbf{A} \cdot \mathbf{I} - g_n \beta_n \mathbf{B} \cdot \mathbf{I} + \mathcal{H}_Q \quad (1)$$

where  $D$  and  $E$  are the axial and rhombic zero-field splitting parameters,  $A$  is the  $^{57}\text{Fe}$  magnetic hyperfine tensor and  $H_Q$  describes the nuclear quadrupole interactions.  $\Delta E_Q = (\epsilon Q V_{zz}/12)(1 + \eta^2/3)^{1/2}$  is the quadrupole splitting, while  $\eta = (V_{xx} - V_{yy})/V_{zz}$  is the asymmetry parameter of the electric field gradient tensor. The shape of the Mössbauer spectrum recorded in an applied field,  $B = 50$  mT (Figure S6), just like the EPR spectrum, indicates that E/D is distributed; we were not able describe the E/D distribution by a symmetric function such as a Gaussian, and therefore we have focused the Mössbauer analysis on the high field spectra ( $B \geq 2$  T), which are essentially independent of E/D. The 8.0 T spectrum reveals that **2** represents at least 95% of total Fe. Importantly, **2** has a negative quadrupole splitting,  $\Delta E_Q = -1.9$  mm/s, the largest value yet observed for a high-spin  $[\text{Fe}^{\text{III}}(\text{TMC})]$  complex.<sup>[8b, 11]</sup> The  $^{57}\text{Fe}$  A tensor of **2** is characteristic of high-spin  $\text{Fe}^{\text{III}}$ . Its isotropic component,  $A_{\text{iso}}/g_n \beta_n = -18.7$  T ( $A_{\text{iso}} = (A_x + A_y + A_z)/3$ ), is comparable to the  $-20.0$  T value reported for the high-spin  $\text{Fe}^{\text{III}}(\text{TMC})(\eta^1\text{-OOH})$  complex,<sup>[8b]</sup> and the smaller value observed for **2** can be attributed to the presence of the more covalent thiolate ligand. Interestingly, the  $D$  and (dominant) E/D values of **2** are quite similar to those observed for  $[\text{Fe}^{\text{III}}(\text{TMC})(\eta^1\text{-OOH})]^{2+}$  ( $D = +2.5$  cm $^{-1}$ , E/D = 0.097).<sup>[8b]</sup> However the isomer shift of **2**,  $\delta = 0.71(3)$  mm/s, is distinctly larger than the  $\delta = 0.51$  mm/s observed for  $[\text{Fe}^{\text{III}}(\text{TMC})(\eta^1\text{-OOH})]^{2+}$ .<sup>[8b]</sup>

The Mössbauer parameters of **2** reveal a high-spin ferric center with unique properties. It has the largest isomer shift for any  $\text{Fe}^{\text{III}}$ -peroxide complex reported thus far,<sup>[8b, 12]</sup> a large and negative  $\Delta E_Q$  (with the largest component of the field gradient along  $z$ ), and an  $^{57}\text{Fe}$  A-tensor that is rather anisotropic for a high-spin  $\text{Fe}^{\text{III}}$  center.<sup>[13]</sup> These three properties have a common origin, as may be inferred from the following considerations. For a high-spin  $\text{Fe}^{\text{III}}$  center, the five d-orbitals are occupied by  $\alpha$  electrons. In order to explain the large and negative  $\Delta E_Q$ , we postulate transfer of  $\beta$  electron density from the two filled peroxo  $\pi^*$  orbitals to the empty  $\beta d_{xz}(\text{Fe})$  and  $\beta d_{yz}(\text{Fe})$  orbitals. If only one orbital were involved ( $d_{xz}$  or  $d_{yz}$ ), a positive  $\Delta E_Q$  would result, with the largest component of the quadrupole tensor in the  $xy$  plane, in contrast to what is observed. However, if  $\beta d_{xz}(\text{Fe})$  and  $\beta d_{yz}(\text{Fe})$  were equally populated, a negative  $\Delta E_Q$  with the major component along  $z$  would result, as observed.<sup>[14]</sup> Since the spin-dipolar contribution to  $^{57}\text{Fe}$  A-tensor is proportional to the valence part of the quadrupole tensor, we expect the donation to increase the magnitude of  $A_z$  and to decrease the magnitude of  $A_{x,y}$ . Indeed, we observe that  $|A_{x,y}| < |A_z|$ . Finally, electron donation by the peroxo ligand into  $\beta d_{xz}$  and  $\beta d_{yz}$  orbitals enhances the d-electron density at the iron, thereby imbuing the iron center with some ferrous character and resulting in an increase in its isomer shift as observed.

X-ray absorption spectroscopy (XAS) provided insight into the structural and electronic properties of **2**. The XAS edge energy of 7123.1 eV observed for **2** falls at the low energy end of the range reported for  $\text{Fe}^{\text{III}}(\text{OO})$  complexes ( $\sim 7123$  to 7125 eV), consistent with an  $\text{Fe}^{\text{III}}$  center ligated by highly basic thiolate and peroxide donors (Figure S8). There is a small pre-edge peak arising from a  $1s \rightarrow 3d$  transition at 7113.6 eV with a peak area of 11.0 units (Table S1), suggesting the presence of a fairly distorted 6-coordinate  $\text{Fe}^{\text{III}}$  center.<sup>[15]</sup>

Analysis of EXAFS data for **2** yielded a principal shell of four N/O scatterers at 2.17 Å, which are attributed to the equatorial nitrogen donors of the TMCS ligand. This distance resembles that for  $[\text{Fe}^{\text{III}}(\text{TMC})(\eta^1\text{-OOH})]^{2+}$  (2.15–2.16 Å) more closely than for its conjugate base  $[\text{Fe}^{\text{III}}(\text{TMC})(\eta^2\text{-OO})]^+$  (2.20–2.23 Å).<sup>[8b, 8c]</sup> The inclusion of an S scatterer at 2.41 Å significantly improved the quality of the fit, indicating coordination of the thiolate moiety to the iron center. However the Fe–S distance found for **2** is rather long, relative to

those observed for other synthetic RS-Fe<sup>III</sup>(OOX) model complexes (~2.30 Å), but comparable to values associated with biological RS-Fe<sup>III</sup>(OOX) intermediates (Table 1). For the peroxy ligand, we considered two possible binding modes,  $\eta^2$ -side-on and  $\eta^1$ -end-on. Attempts to model **2** using an  $\eta^2$ -side-on peroxy moiety yielded unreasonably large  $\sigma^2$  values (>15, Table S2). In contrast, the inclusion of a single O/N scatterer at 1.89 Å significantly improved the quality of the fit (Figure S9 and Table S2). Taken together, the EXAFS fits favor a six-coordinate structure, with a pentadentate TMCS and an  $\eta^1$ -end-on peroxy moiety *trans* to the thiolate ligand.<sup>[16]</sup>

As the RS-Fe<sup>III</sup>( $\eta^1$ -OO<sup>-</sup>) complex would be expected to be prone to protonation, the reactivity of **2** towards weak acids was probed. The addition of 100 equiv. 2,2,2-trifluoroethanol (TFE, pK<sub>a</sub> = 12.5) to a solution of **2** resulted in the rapid (10 s) disappearance of the features assigned to **2** and the formation of new features ( $\lambda_{\text{max}} = 550, 720$  nm) assigned to a new species **3** (Figure S3). Under the same conditions, addition of 100 equiv. of stronger acids such as ammonium acetate (pK<sub>a</sub> = 9.2) or pyridinium triflate (pK<sub>a</sub> = 5.2) also yielded intermediate **3** on the same time scale. In contrast, the reaction between **2** and 100 equiv. MeOH (pK<sub>a</sub> = 15.2) did not yield **3** but instead afforded **1**, presumably due to accelerated decay of KO<sub>2</sub> by disproportionation (Figure S7).

The behavior of **1** with KO<sub>2</sub> is notably different from the RS-Fe<sup>II</sup> complexes studied by Kovacs, for which no reaction with KO<sub>2</sub> was observed until the addition of MeOH, leading to the generation of RS-Fe<sup>III</sup>( $\eta^1$ -OOH) intermediates.<sup>[4a, 4c]</sup> This was true even for the complex of the *N*-(3-mercaptopropyl)cyclam ligand,<sup>[4c]</sup> which is closely related to TMCS. In contrast, superoxide reduction readily occurred in the reaction between **1** and KO<sub>2</sub> in an aprotic solvent, to generate **2**, which could be easily protonated to yield a postulated RS-Fe<sup>III</sup>( $\eta^1$ -OOH) intermediate (**3**) (Scheme S1).

Reactivity studies provided further insights into the properties of the peroxide ligand in **2**. Complex **2** did not react at -90 °C with substrates that contain weak C-H bonds, such as dihydroanthracene, thus demonstrating that the bound peroxy moiety did not possess any electrophilic character. Its nucleophilic nature, however, was demonstrated in its reactivity towards electrophilic substrates. Menadione (2-methyl-1,4-naphthoquinone) is a substrate often used for this purpose, affording menadione epoxide (2,3-epoxy-2-methyl-1,4-naphthoquinone) in high yield (Scheme S2).<sup>[17]</sup> For example, Valentine showed that [Fe<sup>III</sup>(F<sub>20</sub>TPP)( $\eta^2$ -OO)]<sup>-</sup> (F<sub>20</sub>TPP = *meso*-tetrakis(pentafluorophenyl)porphyrinato) did not react with menadione in CH<sub>3</sub>CN at 25 °C but afforded a 70% yield of the epoxide product by change of solvent to dimethyl sulfoxide (DMSO).<sup>[17a, 17c]</sup> The latter reactivity was proposed to result from the binding of DMSO to the Fe<sup>III</sup> center, converting the  $\eta^2$ -side-on peroxy moiety to its  $\eta^1$ -end-on isomer. When **2** was treated with menadione at -90 °C in 4:1 THF/DMF, menadione epoxide was obtained in 100 (±20) % yield within 60 s, supporting the assignment of **2** as an  $\eta^1$ -end-on peroxide complex.

Aldehyde substrates are also useful probes of metal-peroxide nucleophilicity.<sup>[18]</sup> At -90 °C **2** reacted with 20 equiv. of 2-phenylpropionaldehyde (PPA) within 5 s, yielding acetophenone and formate according to GC-MS. Accurate kinetic analysis, and thus determination of second order rate constants ( $k_2$ ), at such rapid rates was not possible; however **2** was clearly a very active reactant for nucleophilic oxidation reactions. UV-vis analysis of the reaction between **2** and PPA (Figure S4) showed isosbestic behaviour and a clean conversion to a new Fe<sup>III</sup> product that displayed features typical of an RS-Fe<sup>III</sup> complex ( $\lambda_{\text{max}} = 480$  nm).<sup>[19]</sup> In stark contrast, we found that [Fe<sup>III</sup>(TMC)( $\eta^2$ -OO)]<sup>+</sup> was not reactive towards PPA at -90 °C in 4:1 THF/DMF, in agreement with Nam's earlier report that side-on [Fe<sup>III</sup>(TMC)( $\eta^2$ -OO)]<sup>+</sup> was not reactive towards PPA at -40 °C.<sup>[8c]</sup> On the other hand, the end-on hydroperoxide analogue [Fe<sup>III</sup>(TMC)( $\eta^1$ -OOH)]<sup>2+</sup> reacted with

PPA over the course of 800 s at  $-40\text{ }^{\circ}\text{C}$ .<sup>[8c]</sup> Based on the accumulated observations on the reactivity of all the above  $\text{Fe}^{\text{III}}(\text{L})(\text{OO})$  complexes, it is clear that **2** contains a very reactive nucleophilic peroxide ligand, which reacts rapidly, even at  $-90\text{ }^{\circ}\text{C}$ . These results further support our assignment of **2** as an  $\text{RS-Fe}^{\text{III}}(\eta^1\text{-OO}^-)$  complex.

In summary, the reaction between an  $\text{RS-Fe}^{\text{II}}$  complex **1** and  $\text{KO}_2$  at  $-90\text{ }^{\circ}\text{C}$  in aprotic solvent generates a reversible adduct **2** that is best described as an  $\text{RS-Fe}^{\text{III}}(\eta^1\text{-OO}^-)$  complex on the basis of its spectroscopic properties. We postulate that **2** represents the first synthetic model of the initial SOR-superoxide adduct prior to its protonation in the SOR catalytic cycle. Two recent DFT studies favor an  $\text{RS-Fe}^{\text{II}}(\text{OO}\bullet)$  description for this adduct using simplified active sites that did not include second sphere residues.<sup>[3d,20]</sup> However our results provide experimental evidence that the isomeric  $\text{RS-Fe}^{\text{III}}(\eta^1\text{-OO}^-)$  complex can be generated and stabilized in an aprotic medium and in fact exhibits an absorption band at 610 nm like that found for the SOR intermediate.<sup>[3]</sup> For **2**, the anionic peroxy ligand may be stabilized in part by the potassium ion introduced through the use of  $\text{KO}_2$ . Related porphyrin- $\text{Fe}^{\text{III}}(\text{OO}^-)$  complexes have been reported, but they do not have an axial thiolate ligand.<sup>[7,21]</sup> **2**, therefore, represents a unique example of a thiolato-iron(III)-peroxy anion model compound that mimics the structure and function of the postulated  $\text{RS-Fe}^{\text{III}}(\eta^1\text{-OO}^-)$  intermediates in SOR and the P450 family. We have also shown that the peroxide ligand on **2** is highly nucleophilic in nature and is readily protonated by weak acids, consistent with a possible role for this species in the SOR cycle. Furthermore **2** reacts rapidly with carbonyl compounds, even at  $-90\text{ }^{\circ}\text{C}$ , making it relevant to the nucleophilic chemistry postulated for corresponding  $\text{RS-Fe}^{\text{III}}(\eta^1\text{-OO}^-)$  intermediates in the catalytic cycles of hemethiolate enzymes such as aromatase and NO synthase.<sup>[18, 22]</sup>

## Supplementary Material

Refer to Web version on PubMed Central for supplementary material.

## Acknowledgments

This work was supported by the US National Science Foundation (grant CHE1058248 to L.Q.) and the US National Institutes of Health (grant EB001475 to E.M. and postdoctoral fellowships to A.R.McD. (GM087895) and K.M.V.H. (GM093479)). XAS data were collected at beamline X3B of the National Synchrotron Light Source at the Brookhaven National Laboratory, which is supported by the U.S. NIH and DOE.

## References

1. a) Nivière, V.; Bonnot, F.; Bourgeois, D. Handbook of Metalloproteins. Messerschmidt, A., editor. Vol. 4 & 5. John Wiley & Sons, Ltd; Chichester, UK: 2011. p. 246-258. b) Pereira AS, Tavares P, Folgosa F, Almeida RM, Moura I, Moura JGG. Eur J Inorg Chem. 2007;2569–2581. c) Kurtz DM Jr. Acc Chem Res. 2004; 37:902–908. [PubMed: 15612680]
2. a) Mathé C, Weill CO, Mattioli TA, Berthomieu C, Houée-Levin C, Tremey E, Nivière V. J Biol Chem. 2007; 282:22207–22216. [PubMed: 17545670] b) Kovacs JA, Brines LM. Acc Chem Res. 2007; 40:501–509. [PubMed: 17536780]
3. a) Lombard M, Houée-Levin C, Touati D, Fontecave M, Nivière V. Biochemistry. 2001; 40:5032–5040. [PubMed: 11305919] b) Mathé C, Mattioli TA, Horner O, Lombard M, Latour JM, Fontecave M, Nivière V. J Am Chem Soc. 2002; 124:4966–4967. [PubMed: 11982354] c) Nivière V, Asso M, Weill CO, Lombard M, Guigliarelli B, Favaudon V, Houée-Levin C. Biochemistry. 2004; 43:808–818. [PubMed: 14730986] d) Bonnot F, Molle T, Ménage S, Moreau Y, Duval S, Favaudon V, Houée-Levin C, Nivière V. J Am Chem Soc. 2012; 134:5120–5130. [PubMed: 22360372] e) Coulter ED, Emerson JP, Kurtz DM Jr, Cabelli DE. J Am Chem Soc. 2000; 122:11555–11556. f) Emerson JP, Coulter ED, Cabelli DE, Phillips RS, Kurtz DM Jr. Biochemistry. 2002; 41:4348–4357. [PubMed: 11914081]

4. a) Shearer J, Scarrow RC, Kovacs JA. *J Am Chem Soc.* 2002; 124:11709–11717. [PubMed: 12296737] b) Krishnamurthy D, Kasper GD, Namuswe F, Kerber WD, Sarjeant AAN, Moenne-Loccoz P, Goldberg DP. *J Am Chem Soc.* 2006; 128:14222–14223. [PubMed: 17076472] c) Kitagawa T, Dey A, Lugo-Mas P, Benedict JB, Kaminsky W, Solomon E, Kovacs JA. *J Am Chem Soc.* 2006; 128:14448–14449. [PubMed: 17090014] d) Namuswe F, Kasper GD, Sarjeant AAN, Hayashi T, Krest CM, Green MT, Moenne-Loccoz P, Goldberg DP. *J Am Chem Soc.* 2008; 130:14189–14200. [PubMed: 18837497] e) Jiang Y, Telser J, Goldberg DP. *Chem Commun.* 2009; 44:6828–6830. f) Namuswe F, Hayashi T, Jiang Y, Kasper GD, Sarjeant AAN, Moenne-Loccoz P, Goldberg DP. *J Am Chem Soc.* 2009; 132:157–167. [PubMed: 20000711] g) Stasser J, Namuswe F, Kasper GD, Jiang Y, Krest CM, Green MT, Penner-Hahn J, Goldberg DP. *Inorg Chem.* 2010; 49:9178–9190. [PubMed: 20839847] h) Nam E, Alokolaro PE, Swartz RD, Gleaves MC, Pikul J, Kovacs JA. *Inorg Chem.* 2011; 50:1592–1602. [PubMed: 21284379]
5. Fiedler AT, Halfen HL, Halfen JA, Brunold TC. *J Am Chem Soc.* 2005; 127:1675–1689. [PubMed: 15701002]
6. As peroxide is a byproduct of superoxide disproportionation, control experiments between **1** and H<sub>2</sub>O<sub>2</sub> or Na<sub>2</sub>O<sub>2</sub> were carried out in THF/DMF at –90 °C. In neither case was a reaction observed over the course of 1 h.
7. a) Duerr K, Macpherson BP, Warratz R, Hampel F, Tuzcek F, Helmreich M, Jux N, Ivanovic-Burmazovic I. *J Am Chem Soc.* 2007; 129:4217–4228. [PubMed: 17371019] b) Duerr K, Jux N, Zahl A, van Eldik R, Ivanovic-Burmazovic I. *Inorg Chem.* 2010; 49:11254–11260. [PubMed: 21058668] c) Duerr K, Olah J, Davydov R, Kleimann M, Li J, Lang N, Puchta R, Hubner E, Drewello T, Harvey JN, Jux N, Ivanovic-Burmazovic I. *Dalton Trans.* 2010; 39:2049–2056. [PubMed: 20148224]
8. a) Annaraj J, Suh Y, Seo MS, Kim SO, Nam W. *Chem Commun.* 2005:4529–4531. b) Li F, Meier KK, Cranswick MA, Chakrabarti M, Van Heuvelen KM, Münck E, Que L Jr. *J Am Chem Soc.* 2011; 133:7256–7259. [PubMed: 21517091] c) Cho J, Jeon S, Wilson SA, Liu LV, Kang EA, Braymer JJ, Lim MH, Hedman B, Hodgson KO, Valentine JS, Solomon EI, Nam W. *Nature.* 2011; 478:502–505. [PubMed: 22031443]
9. a) Yeh AP, Hu Y, Jenney FE, Adams MWW, Rees DC. *Biochemistry.* 2000; 39:2499–2508. [PubMed: 10704199] b) Katona G, Carpentier P, Nivière V, Amara P, Adam V, Ohana J, Tsanov N, Bourgeois D. *Science.* 2007; 316:449–453. [PubMed: 17446401]
10. Kühnel K, Derat E, Terner J, Shaik S, Schlichting I. *Proc Nat Acad Sci USA.* 2007; 104:99–104. [PubMed: 17190816]
11. Berry JF, Bill E, Bothe E, Neese F, Wieghardt K. *J Am Chem Soc.* 2006; 128:13515–13528. [PubMed: 17031965]
12. Costas M, Mehn MP, Jensen MP, Que L Jr. *Chem Rev.* 2004; 104:939–986. [PubMed: 14871146]
13. Lang G. *Quart Rev Biophys.* 1970; 3:1–60.
14. The valence contribution to the principal components of the quadrupole tensor ( $Q'_{xx,yy,zz}$ , in atomic units) is proportional to  $(-2/7, +4/7, -2/7)$  and  $(+4/7, -2/7, -2/7)$  for an electron in  $d_{xz}$  and  $d_{yz}$ , respectively. Adding these contributions yields  $(2/7, 2/7, -4/7)$ . (See Gütllich P, Link R, Trautwein A. *Mössbauer Spectroscopy and Transition Metal Chemistry.* Springer-Verlag Berlin-Heidelberg-New York 1978)
15. DeBeer George S, Petrenko T, Neese F. *J Phys Chem A.* 2008; 112:12936–12943. [PubMed: 18698746]
16. Because of the importance of vibrational information, we made a number of attempts to obtain such data to probe the peroxide binding mode in **2**, but these experiments were all unsuccessful. These experiments are described in the Supporting Information.
17. a) Selke M, Sisemore MF, Valentine JS. *J Am Chem Soc.* 1996; 118:2008–2012. b) Sisemore MF, Burstyn JN, Valentine JS. *Angew Chem Int Ed.* 1996; 35:206–208. c) Selke M, Valentine JS. *J Am Chem Soc.* 1998; 120:2652–2653.
18. Wertz DL, Valentine JS. *Struct Bonding.* 2000; 97:38–60.
19. a) Kennepohl P, Neese F, Schweitzer D, Jackson HL, Kovacs JA, Solomon EI. *Inorg Chem.* 2005; 44:1826–1836. [PubMed: 15762709] b) Bukowski MR, Koehntop KD, Stubna A, Bominaar EL, Halfen JA, Münck E, Nam W, Que L Jr. *Science.* 2005; 310:1000–1002. [PubMed: 16254150]

20. Dey A, Jenney FE, Adams MWW, Johnson MK, Hodgson KO, Hedman B, Solomon EI. *J Am Chem Soc.* 2007; 129:12418–12431. [PubMed: 17887751]
21. Liu JG, Shimizu Y, Ohta T, Naruta Y. *J Am Chem Soc.* 2010; 132:3672–3673. [PubMed: 20196593]
22. a) Akhtar MRCM, Corina DL, Wright JN. *Biochem J.* 1982; 201:569–580. [PubMed: 7092812] b) Korzekwa KR, Trager WF, Smith SJ, Osawa Y, Gillette JR. *Biochemistry.* 1991; 30:6155–6162. [PubMed: 1647815] c) Pufahl RA, Wishnok JS, Marletta MA. *Biochemistry.* 1995; 34:1930–1941. [PubMed: 7531495] d) Woodward JJ, Chang MM, Martin NI, Marletta MA. *J Am Chem Soc.* 2008; 131:297–305. [PubMed: 19128180]

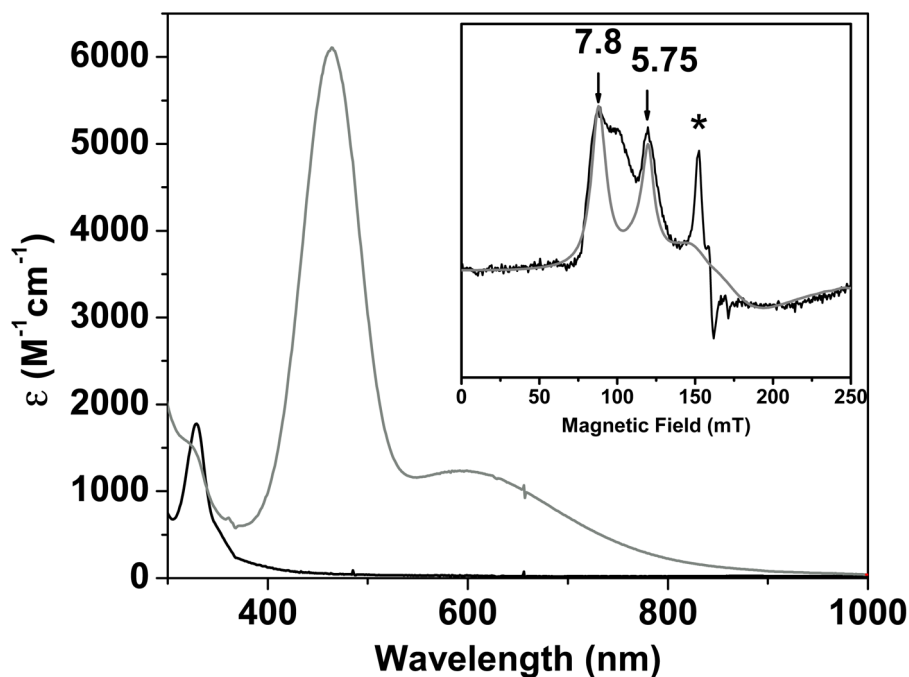


**Figure 1.**

UV-vis spectrum of **1** (black trace, 0.2 mM in 4:1 THF/DMF (v/v) at  $-90$  °C) that reacted with  $KO_2$  to yield **2** (gray trace). Molar absorptivity values were calculated using a combination of UV-vis and Mössbauer experiments. Inset: X-band EPR spectrum of **2** in 4:1 THF/DMF.  $T = 20$  K; microwave power, 2 mW, microwave frequency, 9.645 GHz, modulation amplitude, 10 G, modulation frequency, 100 Hz. Gray line is a theoretical spectrum for an  $S = 5/2$  species with  $E/D = 0.08$ , and  $E/D$  distribution  $\sigma(E/D) = 0.03$  (see text). The sharp feature marked with \* arises from minor ( $\approx 0.5$  % of Fe) contaminant. The high-field region is not shown as it is dominated by the intense absorption of free  $KO_2$ .



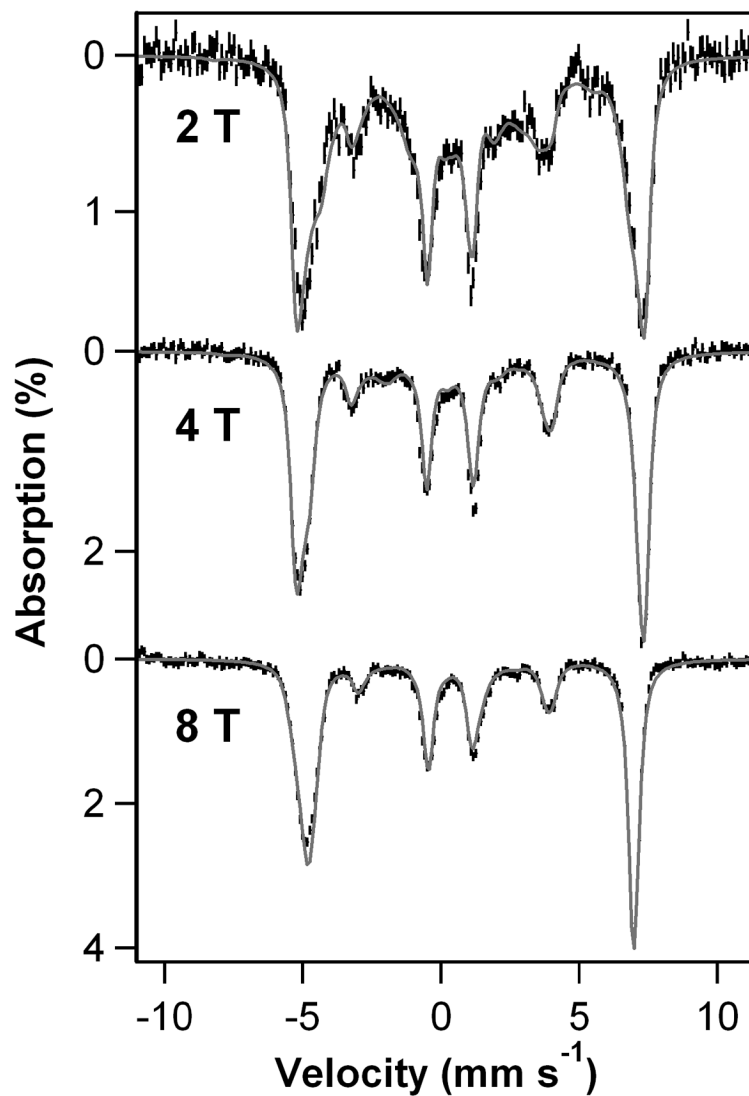
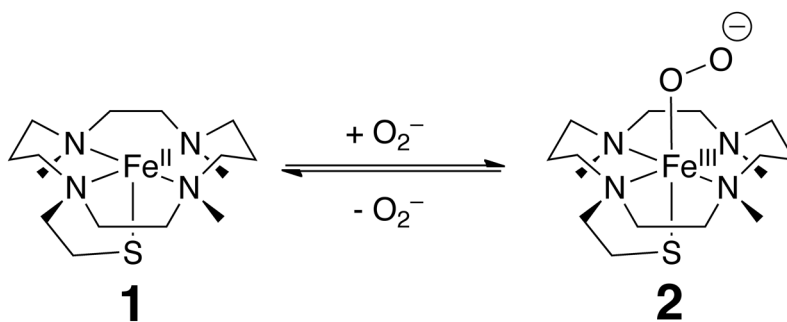


**Figure 2.** 4.2 K Mössbauer spectra of **2** recorded in parallel applied magnetic fields indicated in the figure. The gray curves are spectral simulations using the  $S = 5/2$  spin-Hamiltonian of eq. 1 with  $D = 2.5 \text{ cm}^{-1}$ ,  $E/D = 0.08$ ,  $g_{x,y,z} = 2.0$ ,  $\delta = 0.71(3) \text{ mm/s}$ ,  $\Delta E_Q = -1.9(1) \text{ mm/s}$ ,  $\eta = -0.20$ ,  $A_x/g_n\beta_n = A_y/g_n\beta_n = -17.5(4) \text{ T}$ ,  $A_z/g_n\beta_n = -21.0(5) \text{ T}$ .



**Scheme 1.**  
Equilibrium between **1** and **2**.

**Table 1**Properties of SOR and related RS-Fe<sup>III</sup>(OOX) complexes.

	$\lambda_{\text{max}}$ (nm) (e, M <sup>-1</sup> cm <sup>-1</sup> )	r (Fe-S) (Å)	r (Fe-OO) (Å)
wt-SOR <sub>ox</sub> [RS-Fe <sup>III</sup> (Glu)] <sup>[3c,9a]</sup>	644 (1900)	2.42–2.46	
wt-SOR <sub>red</sub> + superoxide <sup>[3]</sup>	600 (2800)		
E114A-SOR <sub>ox</sub> + H <sub>2</sub> O <sub>2</sub> [RS-Fe <sup>III</sup> (OOH)] <sup>[3b,9b]</sup>	560	2.5	2.0
chloroperoxidase Cpd 0 <sup>[10]</sup>		2.4	1.9
2 [Fe <sup>III</sup> (TMCS)(η <sup>1</sup> -OO <sup>-</sup> )]	460 (6100), 610 (1200)	2.41	1.89
[Fe <sup>III</sup> (cyclam-PrS)-(OOH)] <sup>+ [4c]</sup>	535 (1350)		
[Fe <sup>III</sup> (S <sup>Me</sup> <sub>2</sub> N <sub>4</sub> tren)-(OOH)] <sup>+ [4a,4b]</sup>	452 (2780)	2.33	1.86
[Fe <sup>III</sup> ([15]aneN <sub>4</sub> )(SAr)-(OOR)] <sup>+ [4b,4d]</sup>	~ 525	2.29–2.32	1.82–1.85
[Fe <sup>III</sup> (Me <sub>4</sub> [15]aneN <sub>4</sub> )-(SPh)(OOR)] <sup>+ [4f,4g]</sup>	340 (3500), 405 (2300), 650 (2300)		